A STUDY OF WINDKESSEL MODELS FOR CEREBRAL HEMODYNAMIC CIRCULATION IN HUMANS

Ioana-Corina BOGDAN[1], Takashi TARUMI[2], Dan O. POPA[3]

The purpose of this study was: 1) apply different Windkessel models to the human cerebral circulation, and 2) compare the experimental data. We tested 24 healthy adults between the ages of 22 and 80 years old. The arterial blood pressure and cerebral blood flow velocity were used as the input and output signals during the hemodynamic parameter estimation. The arterial pressure waveform was measured from the common carotid artery while simultaneously recording the cerebral blood flow velocity from the middle cerebral artery using a transcranial Doppler probe with a sampling frequency of 1KHz. Different linear models were studied in the parameter estimation. Results showed that a Box-Jenkins linear model provides good confidence values, and Windkessel model with four elements is closest to expressing cerebral hemodynamic circulation.

Keywords: Age, Hemodynamic circulation and Modeling, Linear Models, Parameter Estimation, Windkessel Model, Peripheral Resistance, Compliance of Vessels, Input impedance.

1. Introduction

In this paper we study lumped models of cerebral hemodynamic circulation and compare them against experimental measurements in adult subjects of different ages. For this study the measurements were collected from 24 subjects. If sufficiently accurate, models may be able to offer clinical indicators of impaired blood flow regulation in the brain under pathophysiological conditions such as aging, neurodegenerative disease, and stroke. Quantitative studies of the cerebrovascular system are not new, and several categories of models have been proposed in past studies. The first category contains a distributed model, frequently used to describe detailed vascular geometry and assuming that the circulatory system is linear. The distributed model is based on circular cylindrical shapes and longitudinal impedance [1]. The second category includes transmission line models or lumped Windkessel (WD) models, where the arterial system considers the mean

[1] Electrical Engineering and Computers Science Department of Electronics and Computers Faculty, University Transilvania of Brasov & CiTi, Romania, e-mail: corina.bogdan@unitbv.ro
[2] Dr., Department of Neurology and Neurotherapeutics, University of Texas Southwestern Medical Center, e-mail: takashi.tarumi@aist.go.jp
[3] Prof. Department of Electrical Engineering, Next Generation Research, Group (NGS), University of Louisville, e-mail: dopopa01@louisville.edu

values of the wave shapes of the pressure and flow and assumes the system to be linear [1]. One of these models is the Broemser model which corresponds to the WD model with three elements [2]. The Toska model is another mathematical expression used for the circulatory system modeling that consists of a heart, an elastic arterial reservoir and two resistive vascular beds disposed in parallel [3]. This model captures cardiovascular changes in humans, beat-to-beat variations and neglects the pulsatile pattern of the flow [2].

Arterial WD model that is applied for a high-frequency pressure-flow relation has not been established for the cerebral circulation in human subjects because of challenges in recording cerebral arterial pressure [4]. Past research assumes the magnitude and the phase of blood pressure versus cerebral blood velocity to be a linear transfer function [4]. Olufsen et al. described the blood flow as being an unsteady effect governed by principles of fluid mechanics [5]. To characterize the blood flow and find a comprehensive model, they used the Navier-Stokes equations related to fluid dynamics, as well as the suitable non-Newtonian relations relevant for the blood [5]. The first and second order lumped models are obtained by applying Laplace transform to one dimensional axisymmetric Navier-Stockes equations ([6]), as well as the residue theory and the solutions applied to Bessel equation.

The research contributions of this paper show that a 4-element WD model is the best fit to correlate the pressure and flow measurements of the cerebral circulation. To our knowledge this is the first time such a model was validated for the cerebral circulation and the key lumped parameters can be identified from the experimental data. We compared data fitting results of several WD models using the state-space linear parameter identification algorithms. Since we did not have prior information with respect to characteristics of the signal noise, we also established that a Box-Jenkins model fit provides the highest confidence.

The article is organized as follows: in section 2 are presented the material and methods, in section 3 are provided the notation and a briefly summary about the 2, 3, and 4-th WD models, as well as the state–space linear models used in the parameter's estimation. The identification method will be described in section 4, where the procedure of parameter estimation, criterion of optimization and transfer functions describing WD models will be given, followed by experimental results presented in section 5. Finally, we present the conclusion of this work.

2. Materials and methods

A. Study Participants

This study used data collected from 24 healthy subjects (12 women and 12 men) between ages of 22 and 80 years old. The subjects were recruited from the Dallas/Fort Worth metropolitan area. Each participant was carefully screened for

cardiovascular and cerebrovascular disease. Hypertension, diabetes mellitus, obesity with a BMI greater than 35 Kg/m², smoking, pregnancy, and presence of cerebrovascular, metabolic, neurologic, and psychiatric history were excluded from this study. In addition, patients with inflammatory disease, brain damage or trauma, hypothyroidism, active alcoholism, or drug consumers were excluded [7]. All subjects gave their written informed consent approved by the Institutional Review Boards of the UT Southwestern Medical Center and Texas Health Presbyterian Hospital of Dallas.

B. Available Data and Acquisition

All data were acquired in an environmentally controlled laboratory. All subjects fasted for >12 hours and abstained from caffeine, alcohol, and intense exercise for >24 hours prior to data collection. Subjects rested in the supine position for >10 minutes before hemodynamic measurements. Brachial cuff blood pressure was taken intermittently using electroshygmomanometer (Suntech, Morrisville, NC, USA). Non-invasive beat-by-beat arterial pressure waveform was recorded from either the common carotid artery (CCA) or the internal carotid artery (ICA) using applanation tonometry (SphygmoCor 8.0, AtCor Medical, Australia). The pencil-type pressure sensor was placed directly on the skin where arterial pulse was felt strongest (see in Fig. 1. the ICA and CCA localizations). Our preliminary observations suggest that pressure waveforms measured in the CCA were like those in the ICA (data not shown). Cerebral blood flow velocity (CBFV) was simultaneously recorded from the middle cerebral artery using transcranial Doppler (TCD) (Multi-Dop X2, Compumedics/DWL, Singen, Germany). A 2-MHz TCD probe was placed over the temporal window using a headgrear (Spencer Technologies, Seattle, WA) and fixated at a constant angle and depth where the optimal CBFV signal was obtained. The data was collected with a sampling frequency of 1KHz.

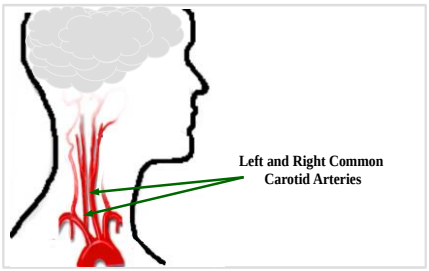

Fig. 1. Human carotid artery.

Carotid pressure waveforms recorded by applanation tonometry was calibrated to brachial blood pressure using a standard procedure described in detail elsewhere [7]. Briefly, beat-by-beat recording of brachial arterial pressure

waveforms was first calibrated to systolic and diastolic brachial blood pressures measured by electroshygmomanometer. Brachial mean arterial pressure was calculated from area under curve of the brachial arterial pressure waveform. Carotid pressure waveform was then calibrated to brachial mean and diastolic blood pressures. More details about this procedure can be found in [7].

3. Windkessel Model Description

A. Windkessel circulatory models

The WD model is a lumped-parameter model applied for the hemodynamic relationship between blood pressure and flow measured through the human vascular system [5], [9], [11]. In the cardiovascular system, it can be used to calculate stroke volume based on the aortic pressure and flow relationship. The WD model was introduced by S. Hales [12-14], formalized mathematically by O. Franck [15-16] considering models consisting of two elements, resistors, and capacitors. [17] extended the WD model to three and four elements respectively, based on the assumption that with the addition of more elements, the model capacities will better represent the pressure-flow relationship, a relation that can be interpreted as an input impedance when the system is linear [12] and the high-frequency behavior is considerably improved [9]. The input impedance provides an accurate description of the arterial tree and is related to the arterial wall properties and blood properties but also to the wave propagation [17].

The WD model has traditionally been used to estimate the hemodynamic load on the heart. The model can be applied to any circulatory system in the human body, including the brain [15]. It is a simple model derived from the Poinseuille's Law developed for the hydraulic system, but in the Windkessel case describes the blood flow through the arteries compared with the fluid flow through pipes [15]. However, this model raises questions on how the arterial tree is properly reflected during the modeling stage and how to manage the estimated arterial properties [9]. Different Windkessel model will be presented below, and its parameters will be estimated using linear models, results shown in section IV.

B. Two-element Windkessel Model

The first WD model has a simple form consisting of two elements (i.e., resister and capacitor) in parallel as shown in the electric analog circuit from Fig. 2(a), [15]. The total resistance R depends on the radius of the vessel, and the compliance of an arterial network C refers to the elasticity of the vessels [17]. R increases with a smaller radius of the vessels while C increases with the elasticity of the vessels.

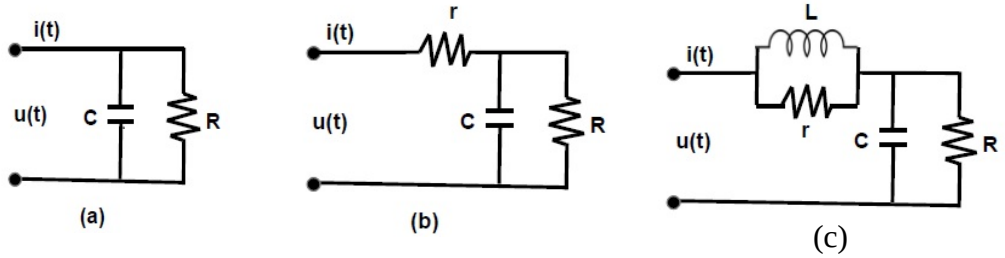

Fig. 2. WD model with two elements (a), three elements (b) and four elements (c)

The model of the arterial bed is described by a differential equation:

$$i(t) = \frac{u(t)}{R} + C\frac{du(t)}{dt} \quad (1)$$

where *i(t)* and *u(t)* are the cerebral blood flow velocity, analogue to the current flowing in the circuit and the carotid blood pressure respectively, which is a time-varying potential [15]. A more detailed description of Fig. 2. is provided elsewhere [15]. Applying Laplace transform to equation (1), we get a first order transfer function of the analogue electric circuit (see equation (2)). This expression will be used in the parameter estimation, R and C respectively.

$$H(s) = \frac{U(s)}{I(s)} = \frac{R}{RCs+1} \quad (2)$$

Based on Fig. (2)(a) the input impedance can be calculated as follows:

$$Z(s) = \frac{R}{RCs+1} \quad (3)$$

There are different types of vascular impedances, but the input impedance quantifies the total sum of resistance and capacitance based on the hemodynamic relation between the blood pressure and flow [10].

C. Three-element Windkessel Model

The second form of the WD model consists of a new element that is the characteristic impedance, r (Fig. 2(b)) [19-22], [33], which provides a liaison between the left ventricle and its after load [12]. The 3-element WD model can generate the same pressure wave profiles as in the arterial tree [11] and capture the dynamics of the cerebral circulation [22]. The model can be described by two equations resulted from the analog electric circuit (see eq. (4) and eq. (5)), and applying Laplace transform to these equations will obtain a transfer function of first order for the equivalent WD model with three elements (see eq. (6)).

$$i(t) = \frac{u_c(t)}{R} + C\frac{du_c(t)}{dt} \quad (4)$$

$$u(t) = i(t)r + u_c(t) \quad (5)$$

Equation (4) is like equation (1), and the characteristic impedance is included in equation (5).

$$H(s) = \frac{RCrs+(r+R)}{RCs+1} \quad (6)$$

The transfer function gives the number of poles and zeros used in the parameter estimation. The input impedance is given by:

$$Z(s) = r + \frac{R}{1+RCs} \quad (7)$$

D. Four-element Windkessel Model

To reduce the errors caused by low frequencies, a WD model was developed with another element, the blood inertia. The 4-element WD model (Fig.2.(c)) was further extended by [1], and the lumped-model has the characteristic resistance r displayed in parallel with the added blood pressure inertia L. Also, the compliance of vessels C remains in parallel with the peripheral resistance R as in the two and three elements Windkessel models. The reasons of developing and extending the WD model were not only to represent a much better pressure flow relationship, but also to better understand the clinical meanings of the estimated parameters [17].

There are three electrical equations resulting from the analog electric circuit, including two differential equations (eq. (9) and eq. (10)) and one equation related to the current that is crossing over the circuit (eq. (8)). After [23], this model provides a relatively good approximation of the real systems and is a better predictor than the other two models [24].

$$u(t) = u_L(t) + r[i(t) - i_L(t)] \quad (8)$$

$$i(t) = i_L(t) + \frac{di_L(t)}{dt} \quad (9)$$

$$\frac{du_c(t)}{dt} = -\frac{1}{RC}u_c(t) + \frac{1}{C}i(t) \quad (10)$$

The transfer function of the WD model is given in equation (11), in which one can be observed that the order is increased becoming a second order transfer function described by two poles at the denominator and two zeros to the numerator. This information will be helpful in the parameter identification and in the selection of the method and tools of parameter estimation.

$$H(s) = \frac{RCLrs^2+L(r+R)s+Rr}{RCLs^2+(L+RCr)s+r} \quad (11)$$

The input impedance of the electric analog circuit is given by the following mathematical expression:

$$Z(s) = \frac{Ls}{1+(L/r)s} + \frac{r}{1+RCs} \quad (12)$$

It should be observed that at low frequencies closer to zero Hz, the input impedance will be near the value of the peripheral resistance, the value corresponding to the

measured mean input flow and pressure rapport. At high frequencies, the input impedance is equal to the characteristic impedance [17].

4. System Identification and Linear Models

The goal of the System Identification is to model the physical system and its dynamics by mathematical expressions based on experimental data that are related to the inputs and outputs of the system. This discipline is extensively used in various applications, including hydrology and medicine [26]. In most cases the system behavior is less known, or the important parameters have limited information, so that the system identification leaves from different types of identification: white box, grey box, or black box. In the present work, the parameter estimation of the WD model uses the black box identification based on linear models: the autoregressive model, the autoregressive moving average model, the output error, and the Box Jenkins method.

The transfer function for each WD model, described by equations (2), (6) and (11) respectively will be associated with a corresponding linear model, having the same degree (equations of first or second order). Knowing the order of the transfer function, based on the input and output measurements we obtain a time domain transfer function with corresponding poles and zeros, which will be converted in frequency domain (s-domain), a transfer function identified with the WD transfer functions. This step will be described in section 5.

A. Autoregressive Model (ARX)

The structure of the ARX Model is given by equation (13). This model is used for a system with an input excitation [27]. In our study, it is represented by blood pressure (BP) measured at the carotid level and is used for its simple estimation algorithm [27], [28].

$$y(t) = \frac{B(q)}{A(q)}u(t - n_k) + \frac{1}{A(q)}e(t) \tag{13}$$

where $A(q) = 1 + a_1 q^{-1} + \ldots + a_{na} q^{-na}$ and $B(q) = b_0 + b_1 q^{-1} + \ldots + b_{nb} q^{-nb}$ are the polynomials of the ARX model, with a_i and b_i constant coefficients that are estimated, and na and nb the degrees of the two polynomials, representing the number of poles and zeros respectively, for the transfer function $B(q)/A(q)$. The input (arterial blood pressure), the output (cerebral blood flow velocity (CBFV)), and the white noise of the system are represented by $u(t)$, $y(t)$ and $e(t)$, and n_k is the backward shift operator usually named delay. Equation (13) translates a sum of transfer functions, the first one generated by the input of the system, and the second one generated by the noise model.

B. Autoregressive Moving Average Models (ARMAX)

The ARMAX model brings the polynomial *C(q)* as an addition to the previous model. By this polynomial, the transfer function generated by the white noise provides a better flexibility to control the disturbance of the system [27].

$$y(t) = \frac{B(q)}{A(q)}u(t - n_k) + \frac{C(q)}{A(q)}e(t) \quad (14)$$

where $C(q) = 1 + c_1 q^{-1} + \ldots + c_{nc} q^{-nc}$ is the noise polynomial term, and c_i are constant coefficients and nc represents the degree of the polynomial.

C. Output Error Model (OE)

A third linear model used in parameter estimation is the OE model (see eq. (14)), where the only uncertainty is the additive white noise *e(t)* [27], a noise generated by the data acquisition procedure.

$$y(t) = \frac{B(q)}{F(q)}u(t - n_k) + e(t) \quad (15)$$

where $B(q)$ keeps the same expression as the ARX model, and $F(q) = 1 + f_1 q^{-1} + \ldots + f_{nf} q^{-nf}$ has a polynomial degree equal to n_f, and f_i are constant coefficients providing the number of zeros of the transfer function $B(q)/F(q)$.

D. Box-Jenkins Model (BJ)

The BJ model includes in its structure the autoregressive, the moving average and the seasonal moving average terms, [29]. The model provides a good flexibility for the transfer function generated by the noise signal, with free polynomials for the numerator and denominator [27].

$$y(t) = \frac{B(q)}{F(q)}u(t - n_k) + \frac{C(q)}{D(q)}e(t) \quad (16)$$

where *B(q), F(q), C(q)* are the same polynomials described previously. The noise denominator transfer function is expressed as: $D(q) = 1 + d_1 q^{-1} + \ldots + d_{nd} q^{-nd}$, with d_i constant coefficients and n_d as the degree of the polynomial.

5. Parameter Estimation

There are different techniques applied in the parameter identification using methods and procedures based on the available data. For input/output data processing, in time or at every moment of time, either a non-recursive or recursive technique of identification can be selected [28]. In this work the parameter identification is obtained using measured data with a sampling period of 1kHz and using a non-recursive technique based on transfer functions.

Previous works in WD model estimation used an automatic procedure for the parameter identification and adopted the Powell algorithm for the optimization

problem. [20] estimates the nonlinear WD model with 3 elements by adding a pressure-dependent compliance; the idea is to separate the linear from the nonlinear part and formulate equations dependent only on resistances even in nonlinear case. In [31] and [11], the lumped model is studied using Matlab computing tools and Simulink environment, which uses the state-space matrices in order to obtain the numerical values of the unknown parameters.

A. Tools and Procedures in Parameter Identification

The strategy of choosing a method follows the theory of WD model if the circulatory system has a linear form. In this case, our model for the pressure-flow relationship will take the form of an ARX, ARMAX, OE or BJ linear model respectively. One example of corresponding profiles to the blood pressure and the blood flow velocity are shown in Fig. 3. The measurements correspond to subject 905, (a female of 32 years old). Using the transfer functions provided by the analog electric circuit for each WD model, we begin the parameter estimation. Looking at eq. (2), which corresponds to the first form of the WD model, the transfer function has a single pole and no zeros. In this case, its transfer function will have only one pole $n_a = 1$ and $n_b = 1$ is not zero because n_b has the orders$B(q) + 1$. Resuming for the other WD models, where there are second order transfer functions, for the model three elements $n_a = 2$, and $n_b = 2$ respectively, and for the model with four elements $n_b = 2$, and $n_b = 3$ respectively.

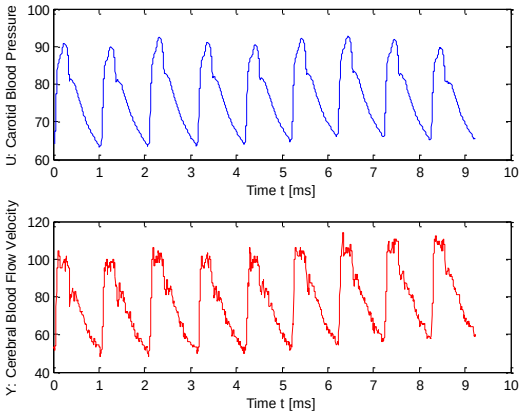

Fig. 3. Comparison of WD model with 2-3-4th elements (Young Subject, female of 32 years old).

The identification of the transfer functions resulted from the available input-output data is obtained using the ***Ident*** toolbox provided by MATLAB, [32].

Few steps are needed in the process of obtaining the proper form of the transfer function. ***Ident*** Toolbox, after declaring the type of linear model, number of poles and zeros, and the transport delay, will provide a discrete transfer function.

Knowing that the input-output data are continuous signals, the discrete transfer function will be converted using the ***d2c*** Matlab function into a continuous transfer function. By testing different transport delays, was observed that the number of zeros of the transfer function will be increased. However, because these zeros are at the origin of the stability plane and do not provide pertinent information, they will be neglected. The optimization criterion used in the ***Ident*** toolbox will be described in the next part, followed by the fitting data related to each WD model.

B. Optimization Criterion

Matlab's ***Ident*** displays the simulated or predicted model output for different domains of input-output validation data (frequency domain, time domain or frequency-response data) [23]. In this case, we are interested in visualizing the time-domain validation data, which is related to the *BestFit* and find the percentage of fitting between the real measurement and the estimation. The *BestFit* represents the optimization criterion for the pressure-flow relation and is calculated using the following mathematical expression:

$$BestFit = \left(1 - \frac{|y-\hat{y}|}{|y-\bar{y}|}\right) \times 100 \tag{17}$$

where y represents the measured output, $\hat{y}$ the simulated or predicted output, and finally$\bar{y}$is the mean of y. The *BestFit* interpretation consider 0% as having no fit ($\hat{y} = \bar{y}$), and 100% as being a perfect fit between the measurement and the estimation. Its value corresponds to a Confidence interval of the output range between 0-100 % probability value that is the output of the system [32].

C. Windkessel Models and Data Fitting

Once all steps mentioned in part *B* of this section are followed, the continuous transfer functions for the three different WD models will have expressions that can be associated with equations (18)-(20). By simple mathematical computing the peripheral resistance, the resistance to blood flow, the compliance of vessels and the blood inertia can be deducted from the estimated coefficients of the denominator and numerator of the transfer functions.

$$H(s) = \frac{R}{sRC+1} = \frac{b_0}{sf_1+f_0} \tag{18}$$

with $C = 1/b_0$and $R = b_0/f_0$, where $b_0, f_0$and $f_1$are the coefficients of the denominator and numerator of $H(s)$, the transfer function corresponding to the WD model with two elements.

$$H(s) = \frac{sRCr+(r+R)}{sRC+1} = \frac{sb_1+b_0}{sf_1+f_0} \tag{19}$$

with $r = b_1$, $C = 1/f_0R$ and $R = (b_0/f_0) - b_1$ where $b_0, b_1, f_0$and $f_1$are the coefficients of the denominator and numerator of $H(s)$, the transfer function corresponding to the WD model with three elements.

$$H(s) = \frac{s^2RCLr+sL(R+r)+Rr}{s^2RCL+s(L+RCr)+r} = \frac{s^2b_2+sb_1+b_0}{s^2f_2+sf_1+f_0} \tag{20}$$

with $r = b_2/f_2$, $L_{1,2} = (f_1 \pm \sqrt{f_1^2 - 4r})/2$, $C_{1.2} = 1/R_1L_{1,2}$ and $R_{1,2} = (b_1/L_{1,2}) - r$, where $b_0, b_1, b_2, f_0, f_1$and $f_2$are the coefficients of the denominator and numerator of $H(s)$, the transfer function corresponding to the WD model with four elements. As it can be observed, there are two different values for the resistance to the blood flow, compliance of blood vessels and blood flow inertia. This is due to a second order equation we have for the numerator of the transfer function. However, in the results only the positive values of these three parameters will be presented for real physiological considerations.

6. Experimental Results

Using the input-output measurements from 24 subjects, the four linear estimation models (i.e., ARX, ARMAX, BJ) for each form of WD model were studied. Three different data set measurements were considered in this study. First, we used the first set of measurements to check the behavior of the linear models and found that delay of 36 ms between changes in blood pressure and blood flow was needed for an accurate estimation of the transfer function coefficients. The meaning of this delay can be interpreted as the time it takes for the blood pressure to travel from the carotid artery to the middle cerebral artery where blood flow is measured. The BJ model provided the best confidence values.

The second set of data was obtained from young subjects and strengthen the idea that BJ model is well fitted as linear model in parameter identification, more than that the linear model shown good confidence values for the 4-WD model. The confidence values for the three different forms of WD model are given in the Appendix, in Table 7. The highest confidence value is obtained in the BJ model applied for 4-WD model being equal to 82.52% (subject 905, woman of 33 years old), and a n_k delay of 24 ms. In the 3 WD model, BJ model provides a confidence value of 78.36% (subject 877, man of 38 years old), and a n_k delay of 16 ms. The confidence value of 3-WD is with almost 5% smaller than the 4-WD model. Based on the results from the two set of data, we proposed to study in the same conditions also old subjects and check if there is any difference between confidences values.

The third set of data was obtained from the same young subjects and from old sub There is a small difference between BJ and OE linear models. In the Appendix are shown the confidence values for all forms of WD model and different linear models for old and young subjects (Tab. 8, Tab. 9). jects this time. Some of the curves fitting of the WD model with two, three and four elements respectively

for young and old subjects (the young subject 857, a woman of 23 years old and an old subject 1057, a man of 72 years old), based on the BJ model can be seen in Fig. 4 and Fig. 5 respectively. It is readily apparent that 2-WD model is not the best choice following the red curve from both figures. The corresponding confidence values for each subject and in function of the WD model forms are given in Tab. 1 and Tab. 2 respectively.

Table 1, Table 2

CONFIDENCE FOR BJ LINEAR MODEL RESULTS FOR WD MODEL, 3RD SET OF MEASUREMENTS, YOUNG SUBJECTS.

Subjects/ Gender/Age	4-WD [%]	3-WD [%]	2-WD [%]
824/M/24	82.3	78.34	57.69
839/F/22	77.85	74.13	47.68
849/F/23	79.03	73.42	54.33
873/M/22	78.84	75.63	64.91
877/M/38	74.42	71.49	58.6
857/F/23	83.84	77.06	48.85
869/F/34	79.42	77.15	44.99
882/M/26	68.15	61.76	37.52
901/M/38	76.85	74.69	64.25
905/F/32	79.18	78.36	63.29
909/F/32	77.74	76.86	53.86
913/M/24	62.8	60.3	50.98

CONFIDENCE FOR BJ LINEAR MODEL Results obtained for WD model, 3rd set OF MEASUREMENTS, OLD SUBJECTS.

Subjects/ Gender/Age	4-WD [%]	3-WD [%]	2-WD [%]
546/M/70	79.62	79.04	41.00
577/M/69	81.69	78.50	58.37
585/M/70	82.07	79.60	62.78
1001/M/70	81.44	78.58	51.91
1003/F/69	77.30	72.94	47.29
1008/F/69	74.59	72.85	42.05
1021/M/71	73.84	73.08	34.77
1022/F/65	78.94	76.42	48.70
1033/F/73	72.84	72.67	64.74
1057/M/72	83.07	78.68	40.05
1059/F/80	82.83	74.39	51.19
1065/F/69	79.10	79.10	55.95

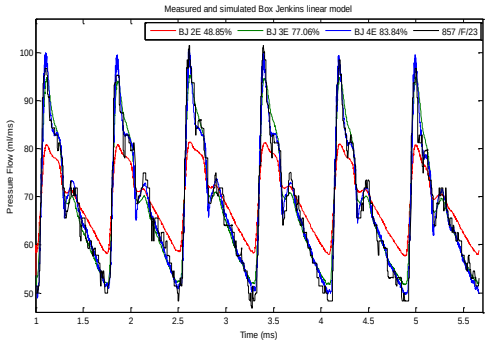

Fig. 4. Comparison of WD with 2-3-4th elements. Data from a representative young subject.

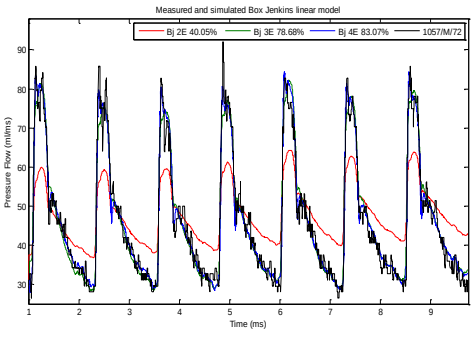

Fig. 5. Comparison of WD with 2-3-4th elements. Data from a representative old subject.

Because 4-WD model provided the highest confidence values than 2-WD and 3-WD model respectively, we proceed to the next step of the study, to the parameter identification. In this case, based on the results obtained in the first and second set

of data, and knowing that BJ linear model describes a complete model with noise properties modeled independent from the system dynamics [35], we decided to estimate the numerical values of the WD model following the BJ results.

In this work the noise model was not considered in the BJ model. Thus, in Tab. 3 and Tab. 4 are given the numerical values for all four parameters based on the BJ linear model. The identified parameters keep the same range of values, (the resistance to the blood and the compliance of vessels have values multiple of $10^3$and 10^{-3}respectively).

The highest confidence value for young subjects was about 84%, and 83% for old subjects which are good fits because the noise of the measurements was not considered, modeled, or filtered. Even in some subjects' case the 3-WD model shows close confidence values to that one with four elements; however, the extended last model provided overall better results. The numerical values obtained for 2-WD and 3-WD are comparable with results found in [5].

Table 3, Table 4

PARAMETERS FOR BJ MODEL, 4-WD
Results: 4-WD, 3rd set of measurements, young subjects.

Subjects/ Gender/ Age	r $[\frac{mm \cdot Hg}{l^{-1} \cdot s}]$	L $[\frac{mm \cdot Hg \cdot l^{-1}}{s^2}]$	R $[\frac{mm \cdot Hg}{l^{-1} \cdot s}] \cdot 10^3$	C $[\frac{l/mm}{Hg}] \cdot 10^3$
824/M/24	1.61	0.04	0.87	27.4
839/F/22	2.86	0.14	0.28	24.8
849/F/23	2.78	0.03	2.03	14.3
873/M/22	2.65	0.05	0.96	18.8
877/M/38	3.19	0.09	0.72	15.5
857/F/23	3.83	0.06	1.43	12
869/F/34	2.46	0.06	0.95	18.7
882/M/26	3.55	0.07	0.8	17.6
901/M/38	1.88	0.03	1.66	18.2
905/F/32	1.53	0.07	0.3	43.8
909/F/32	1.75	0.04	1.18	19.8
913/M/24	1.49	0.03	1.04	28.8

PARAMETERS FOR BJ MODEL, 4-WD
Results: 4-WD, 3rd set of measurements, old subjects.

Subjects/ Gender/Age	r $[\frac{mm \cdot Hg}{l^{-1} \cdot s}]$	L $[\frac{mm \cdot}{Hg \cdot l^{-1} \cdot s^2}]$	R $[\frac{mm \cdot Hg}{l^{-1} \cdot s}] \cdot 10^3$	C $[\frac{l/mm}{Hg}] \cdot 10^3$
546/M/70	1.84	0.02	3.10	13.2
577/M/69	1.54	0.03	1.02	28.1
585/M/70	1.70	0.03	1.53	20.2
1001/M/70	1.62	0.03	0.95	30.3
1003/F/69	1.62	0.03	0.95	30.3
1022/F/65	1.83	0.04	1.08	24.3
1033/F/73	1.58	0.01	5.90	13.1
1057/M/72	2.05	0.08	0.41	32.1
1059/F/80	2.87	0.07	0.70	21.2
1065/F/69	2.11	0.02	5.90	8

7. Conclusion and Future Works

We studied WD models of human cerebral circulation with the increasing number of elements. Based on an assumption of the linear systems, we estimated the Windkessel parameters using the ARX model, ARMAX model, the OE model and BJ model respectively. The hemodynamic data were collected from a group of young adults, and into a next step from old subjects. The third data set allowed us

to conclude that the circulatory hemodynamic can be modeled and estimated using a 4-element model for both young and old subjects. The identified parameters of the model may provide physiological interpretation of effects of aging of the cerebral circulation.

REFERENCES

[1] N. Westerhof and N. Stergiopulos, Models of the arterial tree, Mathematical Modelling in Medicine edited by J.T. Ottesen and M. Danielsen, pp. 65-77, 2000.
[2] S. Kallhovd, Computer modeling of the cardiovascular system and blood pressure regulation, Master Thesis, Faculty of Mathematics and Natural Science, University of Oslo, 2012.
[3] M. Elstad, K. Toska and L. Walloe, Model simulations of cardiovascular changes at the onset of moderate exercise in humans, Journal of Physiology, no.543, issue 2, pp. 719-728, 2002.
[4] R. Zhang, K. Behbehani and B.D. Levine, Dynamic pressure-flow relationship of the cerebral circulation during acute increase in arterial pressure, *Journal of Physics*, vol. 587 (Pt. 11), pp. 2567-2577, 2009.
[5] M. Olufsen and A. Nadim, On deriving lumed models for blood flow and pressure in the systemic srteries, Mathematical Biosciences and Engineering, vol. 1, no. 1, pp. 61-80, 2004.
[6] F. Abraham, M. Behr and M. Heinkenschloss, Shape optimization in unsteady blood flow: a numerical study of non-Newtonian effects, Comput Methods Biomech Biomed Engineering, vol. 8, no. 3, pp. 201-212, 2005.
[7] T. Tarumi, M.A. Khan, J. Liu, M. Tseng, R. Parker, J. Riley, C. Tinahero, R. Zhang, Cerebral hemodynamics in normal aging: central artery stiffness, wave reflection, and pressure pulsatility, *Journal of Cerebral Blood Flow and Metabolism*, vol. 34, pp. 971-978, 2014.
[8] http://www.universityneurosurgery.com/index.php?submenu=ForPatients&src=gendocs&ref=BrainConditions&category=ForPatients
[9] P. Segers, E.R. Rietzschel, M.L. De Buyzere, N. Stergiopulos, N. Westerhof, L.M. Van Bortel, T. Gillebert and P.R. Verdonck, Three and Element Windkessel models: assesment of their fitting performance in a large cohort of healthy middle-aged individuals, *Proceedings of the Institution of Mechanical Engineers*, Part H, vol. 222, issue 4, pp. 417-428, 2008.
[10] Y.S. Zhu, B.Y. Tseng, S. Shibata, B.D. Levine and R. Zhang, Increases in cerebrovascular impedance in older adults, Journal of Applied Physiology, vol. 111, pp. 376-381, 2011.
[11] K. Chellappan, E. Zaheni and M.A. Mohn Ali, Age-related Upper Limb Vascular System Windkessel Model using Photoplethysmography, *3rd Kuala Lumpur International Conference on Biomedical Engineering 2006 IFMBE Proceedings*, vol. 15, pp. 563-566, 2007.
[12] N. Westerhof, J.W. Lankhaar and B.E. Westerhof, The arterial Windkessel, *Medical and Biological Engineering and Computing*, vol. 47, issue 2, pp. 131-141, 2009.
[13] V. Creigen, L. Ferracina, A. Hlod, S. van Mourik, K. Sjauw, V. Rottschafer, M. Vellekoop and P. Zegeling, Modeling Heart Pump, *Proceedings of the 58th European Study Group Mathematics with Industry*, pp. 7-25 ,2007.
[14] J. Aguado-Sierra, J.E. Davies, N. Hadjiloizou, D. Framcis, J, Mayet, A.D. Hughes, K.H. Parker, Reservoir-wave separation and wave intensity analysis applied to carotid arteries: A hybrid 1D model to understand haemodynamics, *Proceedings of the 30th Annual International Conference in Medicine and Biology Society*, pp. 1381-1384, 2008.
[15] M. Catanho, M. Sinha, V. Vijayan, Model of Aortic Blood Flow Using the WD Effect, 2012.
[16] N. Westerhof, N. Stergiopulos and M.I.M. Noble, Snapshots of Hemodynamics: An aid for clinical researcg and graduate education, *Kluvwer Academic Publishers - Dordrecht/Boston/London*, Springer, 2005.

[17] R. Buratini and G. Gnudi, Computer identification of models for the arterial tree input impedance: Comparison between two new simple
models and first experimental results, *Medical and Biological Engineering and Computing*, vol. 20, issue 2, pp. 134-144, 1982.
[18] A. Tsanas, J.Y. Goulermas, V. Vartela, D. Tsiapras, G. Theodorakis, A.C. Fisher, P. Sfirakis, The Windkessel model revisited: A qualitative analysis of the circulatory system, Mechanical Engineering amd Physiscs, no. 31, pp.581-588, 2009.
[19] G. Gnudi, Analytical relationship between arterial input impedance and three-element Windkessel series resistance, *Medical and Biological Engineering and Computing Journal*, vol 36, pp. 480-484, 1998.
[20] A. Cappello, G. Gnudi and C. Lamberti, Identification of the three-element windkessel model incorporating a pressure-dependent compliance, *Annals of Biomedical Engineering*, vol 23, pp. 164-177, 1995.
[21] B. Baumgartner, A. Mendoza, S. Eichhorn, U. Schreiber and A. Knoll, A Comparative study on extra-corporal circulation control, *33rd Annual International Conference of the IEEE EMBS Boston*, Massachusetts USA, pp. 4287-4290, 2011.
[22] P. Gehalot, R. Zhang, A. Mathew and K. Behbehani, Efficacy of Using Mean Arterial Blood Pressure Sequence for Three-Element Windkessel Model Estimation, *28th Annual International Conference in Medicine and Biology Society (EMBS)*, pp. 1379-1382, 2006.
[23] M. Hlavac, Windkessel model analysis in Matlab,
www.feec.vutbr.cz/EEICT/2004/sbornik/03-Doktorske_projekty/01-Elektronika/09-lahvo.pdf
[24] L. Suganthi and M. Manivannan, Effect of Upper Arm Cutt Pressure on Pulse Morphology using Photolethysmography, Procedeeing of the 31st Annual International Conference in Medicine and Biology Society (EMBS), pp. 1792-1795, 2009.
[25] T. Soderstrom and B. Carlsson, Least square parameter estimation of continous time ARX models from discrete-time data, IEEE Transactions on Automatic Control, vol. 42, no.5, pp. 659-673, 1997.
[26] L. Huaiyuan, H. Jianhua and C. Song, Parameter Identification Research based on ARX Model, Applied Mechanics and Materials, vols. 190-191, pp. 292-296, 2012.
[27] I. Kupcina, A, Kopustinskas, Analysis of the arterial compliance estimation using WD models
[28] T.-M. Laleg, M. Sorine and Q. Zhang, Input Impedance of the Arterial System Using Parametric Models, ICES06, 2006.
[29] Z. M. Yusoff, Z. Muhammad, M.H.F. Rahiman and M.N. Taib, ARX Modeling for Down-Flowing Steam distillation, Proceedings of the 8th International Colloquium on Signal Processing and its Application, pp. 485-490, 2012.
[30] http://www.mathworks.com/products/datasheets/pdf/system-identification-toolbox.pdf
[31] L. Ljung, Systems Identification: Theory for the User (2nd Edition), Prentice Hall, 1999.
[32] www.mathworks.com/help/ident/ug/simulating-and-predicting-model output.html#br1fksc-1
[33] D. Garcia and L.-G. Durand, Modeling of the aortic stenosis and systemic hypertension, *Wiley Encyclopedia of Biomedical Engineering*, 2006.
[34] T. Kind, T.J. Faes, J.W. Lankhaar, A. Vonk-Noordegraaf, M. Verhaegen M, Estimation of three and four element windkessel

APPENDIX

Table 7

CONFIDENCE FOR LINEAR MODELS: WD MODEL USING THE 2ND SET OF MEASUREMENTS.

Subjects/ Gender/ Age	4WD [%]				3WD [%]				2WD [%]			
	ARX	ARMAX	OE	BJ	ARX	ARMAX	OE	BJ	ARX	ARMAX	OE	BJ
24/M/24	72.80	72.80	82.30	82.30	72.85	77.06	77.06	77.06	16.11	48.85	48.85	48.85
839/F/22	74.32	76.17	76.17	78.84	73.59	73.59	75.63	75.63	43.72	43.72	64.91	64.91
849/F/23	72.10	72.1	78.62	79.42	72.21	72.21	77.47	77.47	17.33	44.99	44.99	44.99
857/F/23	50.51	50.51	68.15	68.15	50.44	51.66	61.76	61.76	21.42	37.52	37.52	37.52
73/M/22	69.1	76.89	76.89	76.89	68.96	74.73	74.73	74.73	59.53	59.53	64.31	64.31
77/M/38	72.64	79.18	79.18	79.18	72.61	78.36	78.36	78.36	51.12	51.12	63.29	63.29
82/M/26	-40	-40	61.57	61.57	33.96	33.96	21.35	66.65	1.08	19.77	19.77	19.77
01/M/38	64.33	77.74	77.74	77.47	64.39	64.39	76.86	76.86	38.54	38.86	53.86	53.86
905/F/32	58.42	62.80	61.01	62.8	57.72	57.72	60.30	60.30	44.33	44.33	50.98	50.98
906/F/33	72.91	72.91	82.52	82.52	72.68	72.68	78.34	78.34	40.30	57.11	57.69	57.69
909/F/32	67.13	67.13	80.99	80.98	67.36	67.36	74.13	74.13	26.74	26.75	47.68	47.68
913/M/24	65.15	65.15	77.74	79.12	65.18	73.42	73.42	73.42	34.11	54.11	54.11	54.11

Table 8

CONFIDENCE FOR LINEAR MODELS: WD MODEL USING THE 3RD SET OF MEASUREMENTS, YOUNG SUBJECTS.

Subjects/ Gender/ Age	4WD [%]				3WD [%]				2WD [%]			
	ARX	ARMAX	OE	BJ	ARX	ARMAX	OE	BJ	ARX	ARMAX	OE	BJ
819/F/35	69.31	69.31	81.27	81.27	69.31	69.31	79.91	79.91	17.59	17.59	47.83	47.83
824/M/24	72.91	72.91	82.3	82.3	72.68	72.68	78.34	78.34	40.03	40.04	57.69	57.69
839/F/22	67.13	67.13	77.85	77.85	67.36	67.36	74.13	74.13	26.74	26.74	47.68	47.68
849/F/23	65.15	65.15	79.03	79.03	65.18	65.38	73.42	73.42	34.11	34.11	54.33	54.33
873/M/22	72.80	72.8	83.84	83.84	72.85	72.85	77.06	77.06	16.11	16.12	48.85	48.85
877/M/38	67.96	67.96	74.42	74.42	67.73	67.73	71.49	71.49	46.80	46.8	58.6	58.6
857/F/23	74.22	74.22	78.84	78.84	73.59	73.59	75.63	75.63	43.72	43.72	64.91	64.91
869/F/34	72.10	72.1	79.42	79.42	72.21	72.21	77.15	77.15	17.33	17.33	44.99	44.99
882/M/26	50.51	50.51	68.15	68.15	50.44	50.44	61.76	61.76	21.42	21.42	37.52	37.52
901/M/38	69.05	69.05	76.85	76.85	68.91	68.91	74.69	74.69	54.67	54.67	64.25	64.25
905/F/32	72.64	72.64	79.18	79.18	72.61	72.61	79.18	78.36	51.12	51.12	63.29	63.29
906/F/33	33.95	33.95	68.9	68.9	33.90	33.9	66.65	66.65	1.08	1.08	19.77	19.77
909/F/32	64.33	64.33	77.74	77.74	64.39	64.39	76.86	76.86	38.54	38.55	53.86	53.86
913/M/24	58.39	58.39	62.8	62.8	57.72	57.72	60.3	60.3	44.33	44.33	50.98	50.98

Table 9

Confidence for Linear Models: WD model using the 3rd set of measurements, Old Subjects.

Subjects/ Gender/ Age	4WD [%]				3WD [%]				2WD [%]			
	ARX	ARMAX	OE	BJ	ARX	ARMAX	OE	BJ	ARX	ARMAX	OE	BJ
546/M/70	58.35	58.28	79.62	79.62	58.28	58.28	79.04	79.04	21.43	21.43	40.99	41
577/M/69	71.89	81.55	81.69	81.69	76.3	71.92	61.08	78.5	36.67	58.34	53.37	58.37
585/M/70	72.45	79.41	82.07	82.07	72.66	72.66	79.6	79.6	45.57	45.57	62.78	62.78
1001/M/70	71.34	71.34	81.44	78.92	71.69	71.69	78.58	78.58	23.47	23.47	51.91	51.91
1003/F/69	62.92	62.92	77.3	77.3	63.06	65.06	72.94	72.94	25.83	25.83	47.29	47.29
1022/F/65	53.3	53.3	74.59	74.59	53.56	53.56	72.85	72.85	24.97	21.71	42.05	42.05
1033/F/73	56.96	56.96	73.84	73.84	56.98	56.98	73.08	73.08	12.55	12.55	34.77	34.77
1057/M/72	62.8	62.8	78.94	78.94	62.92	62.92	76.42	76.42	26.13	26.13	48.7	48.7
1059/F/80	66.45	66.46	72.84	72.84	66.26	72.67	72.67	72.67	60.68	60.68	64.74	64.74
1065/F/69	70.81	70.81	83.07	83.07	70.87	70.81	78.68	78.68	13.56	13.56	40.04	40.05